NUCLEAR SCIENCE AND TECHNIQUES **25**, 040602 (2014)

Apparatus for determining permeability of hydrogen isotopes in molten-salt

ZENG You-Shi (曾友石),[1,2] WU Sheng-Wei (吴胜伟),[2] QIAN Yuan (钱渊),[2]
WANG Guang-Hua (王广华),[2] DU Lin (杜林),[1,2] LIU Wei (刘卫),[2,*] and XIA Zheng-Hai (夏正海)[3,†]

[1] *University of Chinese Academy of Sciences, Beijing 100049, China*
[2] *Key Laboratory of Nuclear Radiation and Nuclear Energy Technology, Shanghai Institute of Applied Physics, Chinese Academy of Sciences, Shanghai 201800, China*
[3] *CNNC Nuclear Power Operations Management Co., Ltd., Haiyan 314300, China*

(Received February 14, 2014; accepted in revised form March 20, 2014; published online August 11, 2014)

In order to provide data on diffusion coefficients and solubility constants of tritium in molten salts for the critical issue of tritium control in the Thorium Molten Salt Reactor (TMSR) program, a two-chamber permeability apparatus separated by a nickel plate had been developed for determining the permeability of hydrogen isotope in molten salts. Descriptions on the permeability apparatus, experimental procedure and the analytical method for determining the diffusivity and solubility of hydrogen isotope in molten salts were presented in this paper. To assess the performance of the apparatus, the blank tests without molten salt were conducted at 300–700 °C. The results showed that the nickel plate acting as the window for hydrogen isotope permeation in the apparatus seemed to have less effect on experiments of determining the permeability of hydrogen isotope in molten slat at 500–700 °C. Furthermore, the applicability of the apparatus with molten salt was also evaluated experimentally, with test experiments of molten Flinak (LiF-NaF-KF) at 500 °C, 600 °C and 700 °C. Diffusion coefficients and solubility constants of hydrogen in molten Flinak can be derived from those test experiments, which were correlated to $D_{\text{Flinak-H}} = 7.06 \times 10^{-5} e^{-54.9/(R_g T)}$ m^2/s and $S_{\text{Flinak-H}} = 1.67 \times 10^{-7} e^{27.0/(R_g T)}$ mol-H_2/(m^3 Pa).

Keywords: Molten-salt, Permeability, Diffusivity, Solubility, Hydrogen isotope

DOI: 10.13538/j.1001-8042/nst.25.040602

I. INTRODUCTION

Molten salt system is widely involved in nuclear reactor technology as fuel and heat transfer media, due to its advantages of low pressure operation, stability of the liquid under radiation, sufficient thermal conductivity, and resistance to corrosion of the structural materials. Such as, UF_4/ThF_4-based salts were proposed for use in molten salt breeder reactors (MSBRs) [1]. In addition, Flibe, the 2 : 1 molten mixture of LiF-BeF_2, considered as tritium breeding material in fusion reactors, was used in the conceptual designs for High-Yield Lithium Injection Fusion-Energy II (HYLIFE-II) [2] and Force-Free Helical Reactor (FFHR) [3]. Another mixed molten salt comprising LiF, NaF and KF (referred as Flinak) was proposed as heat-transfer fluid of molten salt nuclear reactor [4, 5]. The use of molten salts as fuel solvent or heat-transfer fluid is dependent on their inherent characteristic of tritium production as a fission product, and neutron absorption by lithium in the salts. At high temperatures, tritium diffuses through the structural materials and might escape to the environs in amounts, which requires special consideration in applications [6]. Experimental studies on tritium behavior in molten salts and its permeability through the structural materials were reported [7–15].

In China, researches in the application of molten salts as fuel solvent and heat-transfer fluid for thorium-based molten salt reactor (TMSR) have been launched. This requires data relative to the solubility and diffusivity of tritium in the molten salts, and an apparatus design in this regard being developed. The two-chamber design was applied to determine the hydrogen permeability through the molten salt of Flinak [9], the solubility, diffusivity, and isotopic rate of hydrogen isotopes in Li-Pb [8], and the tritium permeation in Flibe [16]. However, limited data are available on the solubility and diffusivity of hydrogen isotope in molten salts. Also, because of the differences in experiment apparatuses, analytical methods and controls for impurities in the salts, the results in the literatures can hardly be comparable. To obtain the valid data on solubility and diffusivity of hydrogen isotopes in molten salts, one should evaluate performance of the experiment apparatus and analytical method for determining hydrogen isotope permeability in molten salt. In this paper, the permeability apparatus and analytical method based on the two-chamber concept are described, performance and applicability of the permeability apparatus are evaluated with blank tests and molten Flinak test.

II. METHODOLOGY

A. The permeability apparatus

A schematic diagram of the apparatus for permeability determination is shown in Fig. 1(a). The system can be divided into functional parts of the gas supply system, permeation pot and heating system, diagnostics system, and auxiliary components. The gas supply system delivers uniform flows of research grade Ar, H_2 (D_2) or their mixture with adjustable pressures and flow rates. The heater keeps the permeation

* liuwei@sinap.ac.cn
† xiazh@cnnp.com.cn

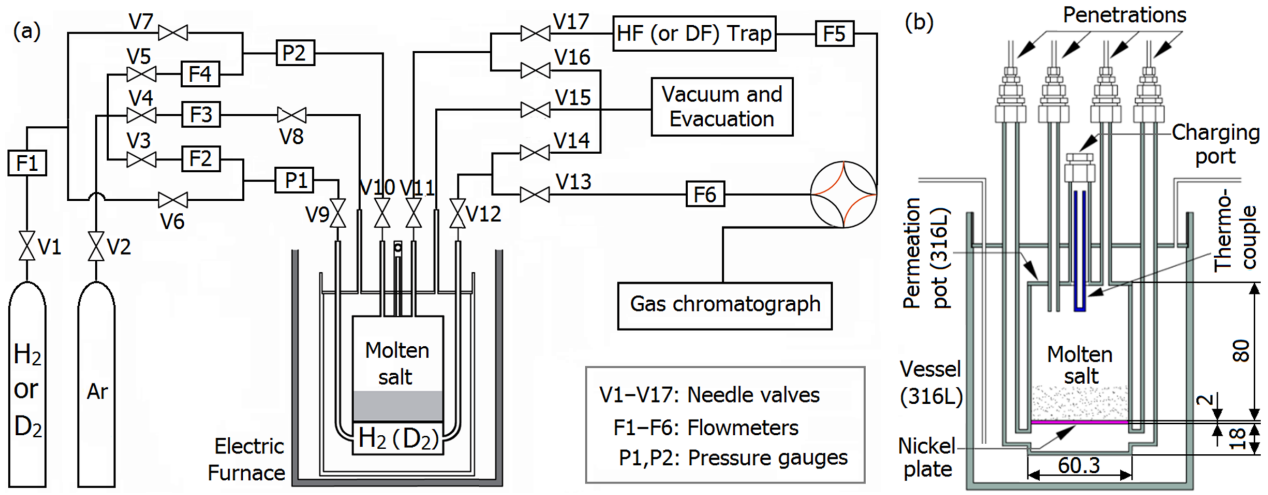

Fig. 1. (Color online) A schematic diagram of the (a) permeability apparatus and (b) permeat pot (dimensions in mm).

pot at a uniform temperature between 500 °C and 700 °C (depending on the molten salt). The diagnostics system is used to measure H_2 concentration in the sweeping Ar gas of the permeate side with a gas chromatographer (Shimadzu model GC-2014 coupled with pulsed discharge helium ionization detector). The auxiliary components include gas delivery systems necessary for experiments, such as gas lines, gas valves, mass flow controllers and pressure gauges.

The permeation pot (Fig. 1(b)) is made of 316L stainless-steel, and separated into two chambers with 2.0-mm thick nickel plate. The 316L stainless-steel and nickel are chosen due to their compatibility with the salts of interest to this work. And the relatively low diffusion coefficient of hydrogen isotopes in 316L stainless-steel at high temperature provides favorable condition for nickel being a good window for hydrogen isotope permeation. Penetrations for the 316L stainless-steel tubing serve as the entrance and exit ports of the experimental gases, the molten salt charging port, and the temperature measurement port with a chromel-alumel thermocouple. The charging port is sealed when the molten salt has been loaded, whereas the temperature measurement port is sealed at the other end (above the molten salt).

The permeation pot is inside a bigger 316L stainless-steel vessel, designed to be argon swept or evacuated to minimize the effects of hydrogen isotope leakage from the permeation pot. Otherwise, H_2 permeating the sidewalls (especially at above 500 °C) into the outer vessel would permeate the sidewall again and return to the inner vessel, causing longer time to approach the steady-state permeation and higher steady-state H_2 concentration in the downstream Ar gas.

B. Experimental procedures

Under argon gas atmosphere of a glove box, the upper-chamber of permeation pot was initially charged with molten salt to yield a known thickness of liquid (in the present case, 20–40 mm) over a specified temperature range. Except when it was impractical to do so, the inner compartment of the chamber is maintained in Ar gas at atmospheric pressure, so as to protect the salt from being dissolved with impurities.

The salt was melted and kept at a required temperature. During the heating period, the outer vessel was swept with an Ar gas flow or evacuated to vacuum by molecular pump. Simultaneously, a purified Ar gas was continuously fed to purge the two chambers. During this period, the Ar gas swept through the surface of molten salt and carried the gas that released from the molten salt into the diagnostic system to measure the H_2 (D_2) concentrations. When the H_2 (D_2) concentration was zero in the upper-chamber, a H_2 (D_2) flow was introduced into the lower-chamber (upstream side) at constant pressure and flow rate. Meanwhile, the Ar gas swept the upper chamber (downstream side) at a constant flow rate (usually $\sim 20\,\mathrm{cm}^3$ (NTP)/min). The H_2 (D_2) having diffused through the molten salt was swept out by the Ar gas and introduced into the diagnostic system for concentration determination, while the diffusivity and solubility in molten salt could be calculated by the one-dimensional diffusion equation, which will be discussed in Sec. II C.

After charging hydrogen isotope into the lower-chamber, a reversal experiment, i.e. charging hydrogen isotope in the upper-chamber was carried out. Under the same operating condition, H_2 (D_2) gas was introduced into the upper-chamber (upstream side) and the permeating H_2 (D_2) was swept out by an Ar flow from the lower-chamber (downstream side). Surface effects between molten salt, nickel plate and hydrogen isotope could be investigated when the direction of hydrogen isotope permeation in molten salt was reversed.

C. Theoretical analysis

Figure 2 shows graphically typical models of hydrogen isotope permeation in molten salt : Model a (Fig. 2(a)) for atom (ion) migration of hydrogen isotopes and Model b (Fig. 2(b))

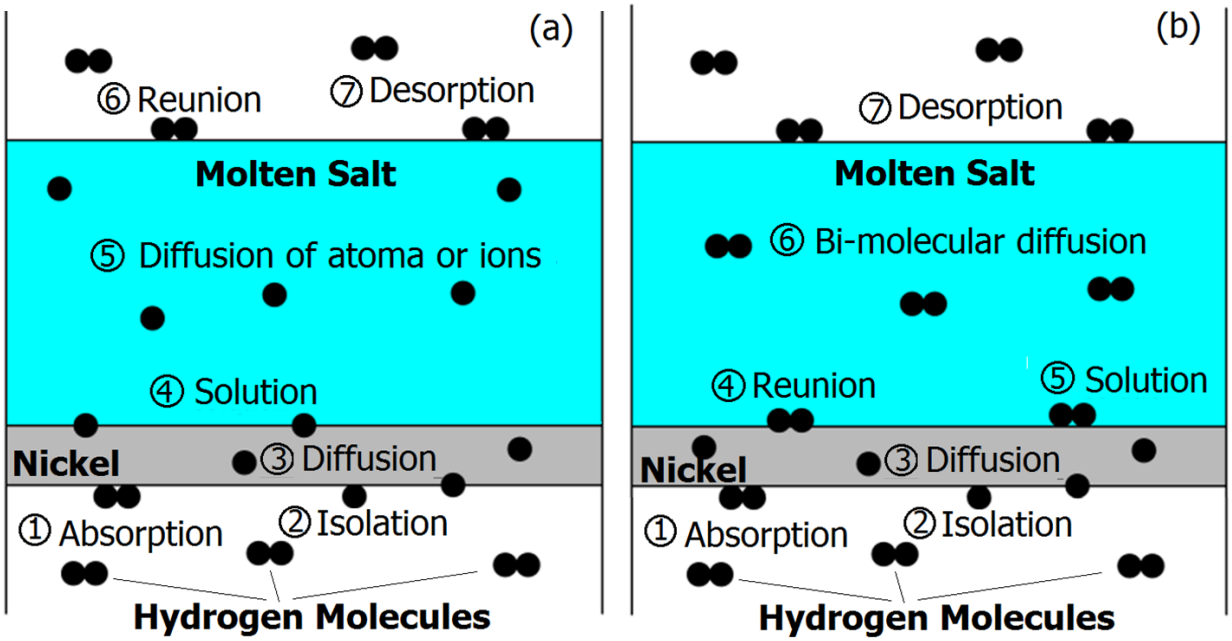

Fig. 2. (Color online) Typical permeation models of H_2 (a) and D_2 (b) in nickel and molten salt system.

for molecule migration of hydrogen isotopes. The transport mechanism of hydrogen isotope in molten salt depends on condition of the salt. In molten Flibe, deuterium and tritium were diffusing as the D^+ and T^+ species [10]. In molten Flinak, hydrogen diffused as a molecular form of H_2, and the H^+ ion diffused under a certain amount of free fluorine ions in the slat [9]. In liquid Li-Pb, the diffusion behavior of hydrogen was based on a binding interaction of Li-H (the charge state of hydrogen was close to H^-) and the dissolved hydrogen atom [17].

The transport process considered in the two models can be described by one-dimensional diffusion equation comprising nickel and molten salt:

$$\frac{\partial c_i}{\partial t} = D_i \frac{\partial^2 c_i}{\partial x^2}, \tag{1}$$

where, subscript i denotes nickel or molten salt; c_i and D_i are molar concentration (in mol/m^3) and diffusivity (in m^2/s) of hydrogen isotope, respectively; x is distance (in m) at the direction of perpendicular to the nickel plant; and t is time (in s).

This is based on assumptions that the overall hydrogen isotope permeation is under diffusion-limiting condition, and the permeation resistance of the nickel plate is much smaller than that of the molten slat. The assumptions were verified by experiments with molten salts of Flinak and Flibe using the same permeability apparatus design [9, 16].

In the present work, the initial and boundary conditions were as follows:

$$t = 0 : c_{\mathrm{Ni}} = 0, c_{\mathrm{molten}} = 0, \tag{2}$$

$$x = 0 : c_{\mathrm{Ni}} = c_{\mathrm{Ni},0} = k_{\mathrm{Ni}} P_{\mathrm{up}}^{1/2}, \tag{3}$$

$$\begin{aligned} &x = L_{\mathrm{Ni}} : c_{\mathrm{Ni}} = c_{\mathrm{Ni},s} = k_{\mathrm{Ni}} P_s^{1/2}, \\ &c_{\mathrm{molten}} = c_{\mathrm{molten},s} = k_{\mathrm{molten}} P_s^{1/2} \quad (\text{Model a}), \\ &c_{\mathrm{molten}} = c_{\mathrm{molten},s} = k_{\mathrm{molten}} P_s \quad (\text{Model b}), \end{aligned} \tag{4}$$

$$x = L_{\mathrm{Ni}} + L_{\mathrm{molten}} : j = W \frac{P_{\mathrm{down}}}{A P_0} = -D_{\mathrm{molten}} \frac{\partial c_{\mathrm{molten}}}{\partial x}, \tag{5}$$

where, subscript i denotes nickel or molten salt; L_i is thickness (in m); k_i is solubility constant (in mol/(m^3 Pa$^{1/2}$) or mol/(m^3 Pa)); P is pressure (in Pa) of hydrogen isotope; W is mole flow rate (in mol/s) of purging gas; A is cross-section (in m^2); and j is permeation flux (in mol/(m^2 s)) of hydrogen isotope.

Then, the solutions of Eq. (1) for steady-state permeation flux (j_{steady}) of hydrogen isotope at the molten salt surface can be written as:

$$j_{\mathrm{steady}} = \frac{D_{\mathrm{molten}} \cdot k_{\mathrm{molten}}}{L_{\mathrm{molten}}} \left(\sqrt{P_{\mathrm{up}}} - \sqrt{P_{\mathrm{down}}} \right) \quad (\text{Model a}), \tag{6}$$

$$j_{\mathrm{steady}} = \frac{D_{\mathrm{molten}} \cdot k_{\mathrm{molten}}}{L_{\mathrm{molten}}} (P_{\mathrm{up}} - P_{\mathrm{down}}) \quad (\text{Model b}). \tag{7}$$

And the solutions to Eq. (1) for transient permeation flux (j_{tra}) can be expressed as:

$$\begin{aligned} &\frac{j_{\mathrm{tra}} \cdot L_{\mathrm{Molten}}}{D_{\mathrm{Molten}} \cdot k_{\mathrm{Molten}} \left(\sqrt{P_{\mathrm{up}}} - \sqrt{P_{\mathrm{down}}} \right)} \\ &= \sqrt{\frac{4L_{\mathrm{Molten}}^2}{\pi \cdot D_{\mathrm{Molten}} \cdot t}} \sum_{n=1}^{\infty} \exp \left[-\frac{(2n-1)^2 L_{\mathrm{Molten}}^2}{4 D_{\mathrm{Molten}} \cdot t} \right] \quad (\text{Model a}), \end{aligned} \tag{8}$$

$$\frac{j_{\text{tra}} \cdot L_{\text{Molten}}}{D_{\text{Molten}} \cdot k_{\text{Molten}}(P_{\text{up}} - P_{\text{down}})} = \sqrt{\frac{4L_{\text{Molten}}^2}{\pi \cdot D_{\text{Molten}} \cdot t}} \sum_{n=1}^{\infty} \exp\left[-\frac{(2n-1)^2 L_{\text{Molten}}^2}{4D_{\text{Molten}} \cdot t}\right] \quad \text{(Model b)}. \tag{9}$$

By fitting the variations of transient permeation flux with time using Eqs. (8) or (9), the diffusion coefficient of hydrogen isotopes in molten salt can be determined independently. In addition, the value of $D_{\text{Molten}} \cdot k_{\text{Molten}}$ can be determined by Eqs. (6) or (7). As a result, the solubility constant of hydrogen isotopes in molten salt can be obtained.

III. RESULTS AND DISCUSSION

A. Permeation measurements without molten salt

H_2 permeation through Ni plate of the apparatus without molten salt was investigated at 300–700 °C. Its purpose was to verify performance of the permeability apparatus, and to measure the diffusivity and solubility of hydrogen isotopes in nickel plate for further comparing the permeation resistance of the nickel plate with that of molten slat layer.

The experiments were conducted by charging hydrogen in the lower-chamber (upstream) under 1.01×10^5 Pa at the flow rate of 20 SCCM (standard-state cubic centimeter per minute). The upper-chamber (downstream) were swept with the Ar flows under 1.01×10^5 Pa, at flow rates and temperatures of 20 SCCM, 300 °C; 20 SCCM, 400 °C; 50 SCCM, 500 °C; 80 SCCM, 600 °C; and 100 SCCM, 700 °C. Simultaneously, the outside vessel was evacuated to vacuum.

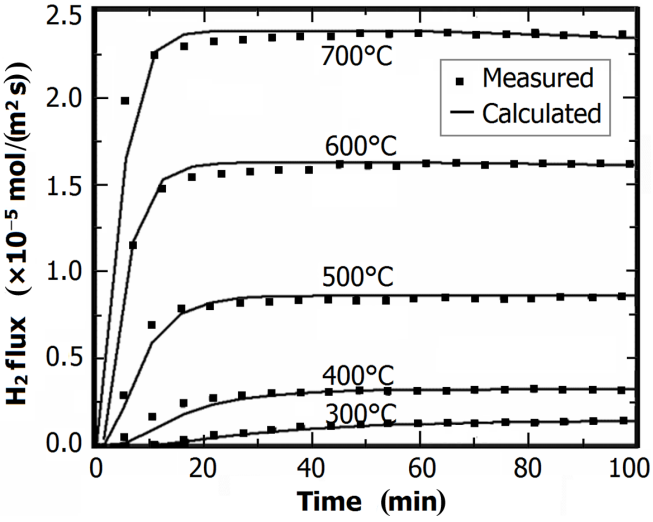

Fig. 3. H_2 molar flux permeated from the Ni plate.

Figure 3 shows the H_2 flux permeated from the nickel plate. The data in squares are from the experiment, while the cureves are from numerical calculations using Eq. (1) and replacing the molten salt to nickel. The calculation results agree well with the experimental results at each temperature.

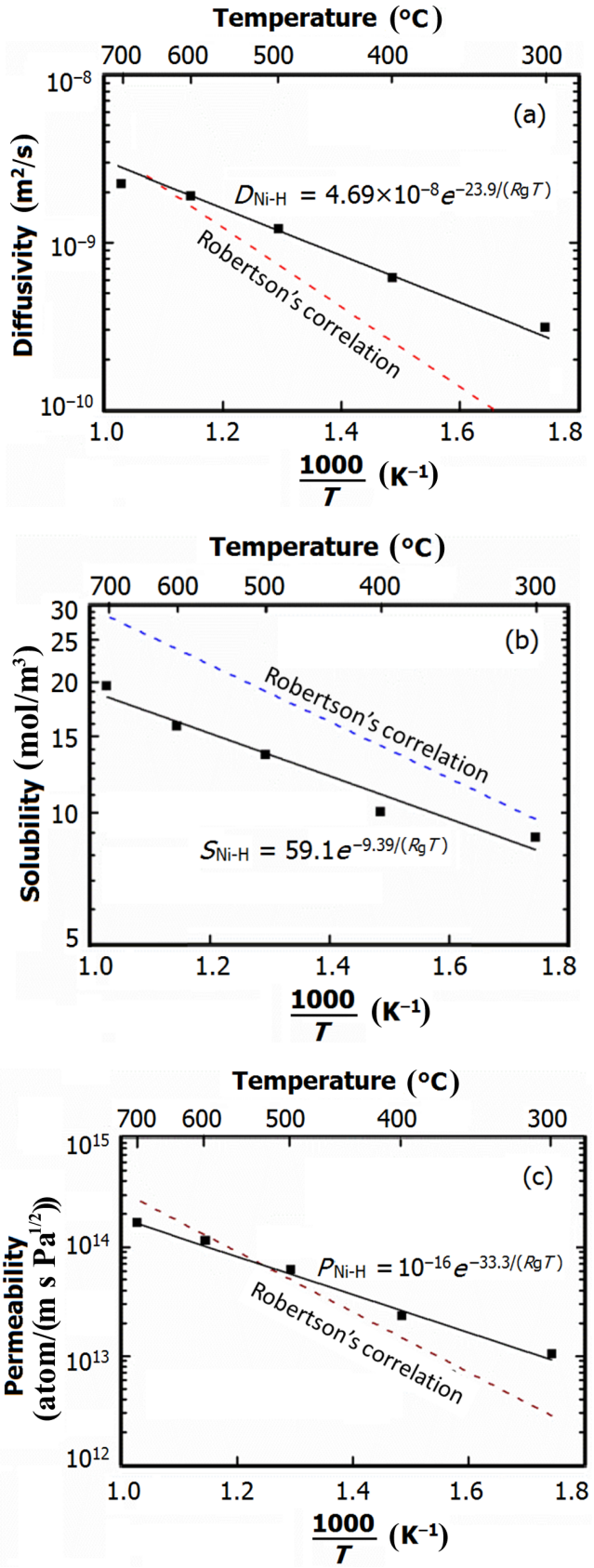

Fig. 4. (Color online) The diffusivity, solubility and permeability of H_2 in Ni.

Fitting the data in Fig. 3, the diffusivity and solubility were determined from the H_2 molar flux curve. Thus, the value of $D_{\text{Ni-H}} \cdot S_{\text{Ni-H}}$, i.e. the H-permeability in nickel, was obtained.

The measured diffusivity, solubility and permeability values are plotted in Fig. 4, where the data could be correlated to the following Arrhenius equations:

$$D_{\text{Ni-H}} = 4.69 \times 10^{-8} e^{-23.9/(R_g T)} \text{m}^2/\text{s}, \quad (10)$$

$$S_{\text{Ni-H}} = 59.1 e^{-9.39/(R_g T)} \text{mol/m}^3, \quad (11)$$

$$P_{\text{Ni-H}} = 1.0 \times 10^{-16} e^{-33.3/(R_g T)} \text{atom/(m s Pa}^{1/2}). \quad (12)$$

For comparison, Robertson's correlations [18, 19] of H-diffusivity, H-solubility and H-permeability in nickel were plotted in Fig. 4. It can be seen that our diffusion results are comparable with Robertson's ones at $> 500\,^\circ$C, but deviate greatly at 300 °C and 400 °C. The solubility in this work is smaller than the published data at 300–700 °C. And the deviation increases with the temperature. This might be caused by surface oxide film of the nickel plate, which can be formed in the Ni plate welding. That fact that the measured diffusivity and solubility can be correlated to Arrhenius equation proves the permeability apparatus meets basic requirements for determining permeability of hydrogen isotopes in molten salt. At 500–700 °C, the H_2 permeability through the Ni plate is in close agreement with the reference data, indicating that the permeability apparatus can be applied at the working temperatures for molten salt.

B. Test with molten Flinak

Experiments were conducted on the apparatus for determining H_2 permeability in molten Flinak at 500 °C, 600 °C and 700 °C. Figure 5 shows H_2 concentrations in the downstream Ar flow as a function of time. The curves (the red lines) calculated by adjusting the H-diffusivity and H-solubility in Eqs. (6)–(9) agree well with the experimental data for all experiment conditions except a small deviation occurred at 500 °C. The disagreement might be due to the effects of hydrogen ion (H^+) diffusion in molten Flinak at 500 °C, which could be caused by the mass-transfer processes at the interfaces between Ni and molten Flinak, and between Ar gas and molten Flinak or impurities in the molten Flinak. However, the effects of H^+ diffusion were limited to the lower temperature of the molten Flinak, while hydrogen diffusion in molten Flinak at higher temperatures were mainly as the molecular form of hydrogen. Despite the small deviation at 500 °C, the test results indicated that the permeability apparatus and the analytical method are applicable for determining the hydrogen isotope permeation in molten salts at 500–700 °C.

In Table 1, the H-diffusivity and H-solubility in molten Flinak measured at 500 °C, 600 °C and 700 °C are compared with the data by Fukada and Morisaki [9]. And our data can be correlated to Eqs. (13) and (14):

$$D_{\text{Fliank-H}} = 7.06 \times 10^{-5} e^{-54.9/(R_g T)} \text{m}^2/\text{s}, \quad (13)$$

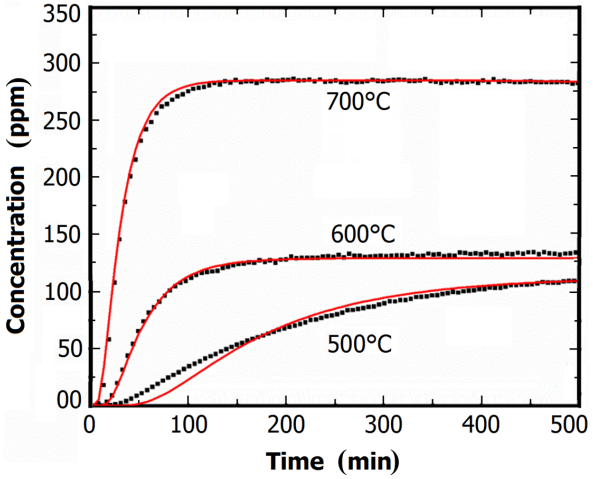

Fig. 5. (Color online) Concentrations in the downstream as a function of Ar gas flow time, at 101 kPa and $L_{\text{Fliank}} = 30$ mm.

TABLE 1. H-diffusivity and H-solubility in molten Flinak

Temperature (°C)	$D_{\text{Fliank-H}_2}$ (10^{-8} m^2/s)		$k_{\text{Fliank-H}_2}$ (10^{-5} mol-H$_2$/(m^3 Pa))	
	This work	Ref. [9]	This work	Ref. [9]
500	1.27	0.18	1.34	15.1
600	4.31	0.99	0.45	4.45
700	7.22	1.71	0.59	3.57

$$S_{\text{Fliank-H}} = 1.67 \times 10^{-7} e^{27.0/(R_g T)} \text{mol/(m}^3 \text{ Pa}). \quad (14)$$

However, the H-diffusivity and H-solubility in molten Flinak measured at 500 °C, 600 °C and 700 °C differ greatly from the data of Ref. [9]. This may be due to the following reasons. The impurity content in molten Flinak, depending on the molten salt and the experiment conditions, can chemically react with H^+ and change the interaction energy between hydrogen and its neighbor molecules in the molten salt, hence the different H-diffusivities and H-solubilities under different experimental conditions. Further investigations are needed, and more tests with hydrogen and deuterium in molten Flinak are in progress at 500–700 °C.

IV. CONCLUSION

Application of fluorine salts as the fuel solvent and the heat-transfer fluid for the Thorium Molten Salt Reactor (TMSR) currently conducted in China has a serious issue with tritium, which is produced at high rates in molten salt and causes permeation leakage and structural material corrosion. A two-chamber apparatus has been developed for determination of permeability of hydrogen isotope in molten salt, which is based on the requirement for data relative to the solubility and diffusivity of tritium in the fluorine salts. The present paper provides the detailed descriptions on the developed permeability apparatus, experimental procedures and the analytical method for determination the diffusivity and solubility of hydrogen isotope in molten salt.

The performance of the experiment apparatus and analytical method that used for determination of hydrogen isotope permeability in molten salt was evaluated with blank tests. It was shown that the nickel plate which acted as the window for hydrogen isotope permeation in the apparatus seemed to have less effect on experiments of determining the permeability of hydrogen isotope in molten slat at 500–700 °C. The applicability of the apparatus with molten salt was also evaluated experimentally, with test experiments of molten Flinak (LiF-NaF-KF) at 500 °C, 600 °C and 700 °C. Diffusion coefficients and solubility constants of hydrogen in molten Flinak can be derived from those test experiments, which were correlated to $D_{\text{Flinak-H}} = 7.06\times10^{-5}e^{-54.9/(R_{\text{g}}T)}$ m^2/s and $S_{\text{Flinak-H}} = 1.67\times10^{-7}e^{27.0/(R_{\text{g}}T)}$ mol-H_2/(m^3 Pa). However, there is a large discrepancy in H-diffusivity and H-solubility in molten Flinak between our data and the previous ones. This may be affected by the impurities included in molten salt, which needs to be further investigated.

[1] Grimes W R. Nucl Appl Technol, 1970, **8**: 137–155.
[2] Moir R W, Bieri R L, Chen X M, *et al*. Fusion Technol, 1994, **25**: 5–25.
[3] Sagara A, Motojima O, Watanabe K, *et al*. Fusion Eng Des, 1995, **29**: 51–56.
[4] Hoffman H W. ORNL Technical Report, CF-53-8-106, 1953.
[5] Sherman S R. 2005 DOE H_2 Annual Review, Project ID # PD31, 2005.
[6] Briggs R B. Reactor Technol, 1971–1972, **14**: 335–342.
[7] Fukada S. J Plasma Fusion Res SERIES, 2013, **10**: 22–26.
[8] Maeda Y, Edao Y, Yamaguchi S, *et al*. Fusion Sci Technol, 2008, **54**: 131–134.
[9] Fukada S and Morisaki A. J Nucl Mater, 2006, **358**: 235–242.
[10] Anderl R A, Fukada S, Smolik G R, *et al*. J Nucl Mater, 2004, **329–333**: 1327–1331.
[11] Nishimura H, Suzuki A, Terai T, *et al*. Fusion Eng Des, 2001, **58–59**: 667–672.
[12] Suzuki A, Terai T, Tanaka S. J Nucl Mater, 1998, **258–263**: 519–524.
[13] Terai T, Suzuki A, Tanaka S. Fusion Technol, 1996, **30**: 911–915.
[14] Terai T, Suzuki A, Tanaka S. J Nucl Mater, 1997, **248**: 159–164.
[15] Reimann J. Fusion Eng Des, 1991, **14**: 413–425.
[16] Calderoni P, Sharpe P, Hara M, *et al*. Fusion Eng Des, 2008, **83**: 1331–1334.
[17] Masuyama D, Oda T, Fukada S, *et al*. Chem Phys Lett, 2009, **483**: 214–218.
[18] Robertson W E. Z Metallkd, 1973, **64**: 436–443.
[19] Reiter F, Forcey K S, Gervasini G. EUR-15217-EN, 1993.